PTECH 2009 - 7th INTERNATIONAL LATIN-AMERICAN CONFERENCE ON POWDER TECHNOLOGY

Zeolite-iron oxide magnetic nanocomposite as a new adsorbent for removal of reactive orange 16 from aqueous solution

Terezinha Elizabeth Mendes de Carvalho[1,a], Denise Alves Fungaro[1,b], Mitiko Yamaura[1,c]

[1]Instituto de Pesquisas Energéticas e Nucleares (IPEN – CNEN/SP), Centro de Química e Meio Ambiente, Av. Professor Lineu Prestes, 2242, São Paulo-SP, Brasil, CEP: 05508-000,
[a]terezinha.de.carvalho@gmail.com, [b]dfungaro@ipen.br, [c]myamaura@ipen.br

Keywords: magnetic adsorbent; zeolite; coal fly ashes; adsorption; reactive orange 16

Abstract. In this work the adsorption features of synthetic zeolite and the magnetic properties of iron oxides have been combined in a composite to produce a magnetic adsorbent. This magnetic composite can be used to adsorb contaminants in water and can subsequently be removed from the medium by a simple magnetic process. The zeolite-iron oxide magnetic composite was prepared by mixing zeolite synthesized from coal fly ashes with magnetite nanoparticles in suspension. The zeolite-iron oxide with weight ratio of 3:1 presented superparamagnetic behavior and was characterized by X-ray diffraction (XRD), surface area (BET-N_2), magnetization measurements, Fourier transform infrared (FTIR) and X-ray fluorescence (XFR) analyses. Batch tests were carried out to investigate the adsorption mechanism of azo dye reactive orange 16 from aqueous solution onto magnetic composite. The dye adsorption equilibrium was attained with 300 min of contact time. Kinetic studies showed that the adsorption process obeyed the pseudo-second-order kinetic model. Adsorption isotherms were analyzed using Freundlich and Langmuir equations. The adsorption equilibrium data fitted well to the Langmuir equation with maximum adsorption capacity of 1.06 mg/g.

Introduction

Adsorption is an important method employed in water treatment with high removal efficiency and low costs. Many kinds of adsorbents have been developed for the removal of

pollutants from water. Magnetic separation is also a promising technology employed in water treatment because of the high separation rate using a simple magnetic process. One example of this technology is the use of magnetite particles to accelerate the coagulation of sewage [1]. It seems attractive to combine adsorption properties with magnetic properties to produce novel kinds of adsorbents for the removal of pollutants from water. After the adsorption is carried out, the adsorbent can be separated from the medium by a simple magnetic process [2, 3].

Some examples are the use of activated carbon/iron oxide magnetic composites for the adsorption of volatile organic compounds [4], montmorillonite–iron oxide magnetic composites for the adsorption of metal cations [5] and NaY zeolite- iron oxide magnetic composite for removal of metallic contaminants from aqueous solution [6].

Zeolite synthesized from Brazilian coal fly ashes offer an attractive and inexpensive material option for removal of contaminants [7-10].

Fly ashes are produced by burning of coal in coal-fired power plants and are the industrial byproduct most generated in southern Brazil: about 4 millions tones/year. Only 30% of this total is reused, mainly for construction purposes. Thus continuous research is needed to develop an alternative technology for utilizing coal ashes.

It is possible to convert fly ash into zeolitic products by hydrothermal treatment with alkaline medium [11-16]. The treated product has a significantly increased surface area and cation exchange capacity when compared to the raw ash.

The objective of this work was to develop a new kind of magnetic adsorbent which can be effective for the removal of anionic reactive azo dye from aqueous solution. For this purpose, the adsorption properties of zeolite synthesized from coal fly ashes were combined with the magnetic properties of iron oxides to produce zeolite-iron oxide magnetic composite. Batch kinetic experiments were performed to provide appropriate equilibrium times. The Langmuir and Freundlich isotherm models were used to model the isotherm data for their applicability.

Materials and Methods

Materials

All chemicals used in this study were of analytical grade. Reactive Orange 16 (RO16), which was used as a model reactive dye in this work, was purchased from Sigma–Aldrich (50% purity). A stock solution was prepared in deionized water (Millipore Milli-Q), and the solutions for adsorption tests were prepared by diluting. The sample of fly ashes from baghouse filter was obtained from a coal-fired power plant located at Figueira City, in Paraná State, Brazil. As shown in

Fig. 1, RO16 has two sulfonate groups, which have negative charges in aqueous solution. The general characteristics of RO16 are summarized in Table 1.

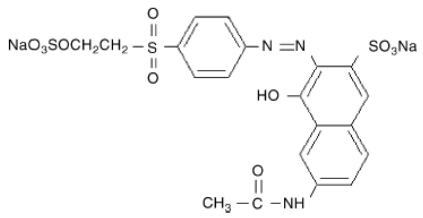

Figure 1. Chemical structure of Reactive Orange 16.

Table 1. General characteristics of RO16

Chemical Formula	$C_{20}H_{17}N_3Na_2O_{11}S_3$
Molar Mass	617.54
Color index Number	17757
λ_{max} (nm)	493

Methods

Characterization techniques

The chemical composition was determined by a RIX-3000 Rigaku X-ray fluorescence spectrometer (XFR). The surface area was determined by N_2 adsorption isotherm using NOVA 1200 (Quantachrome Corp.). The phases of the zeolite were determined by XRD analyses with an automated Rigaku multiflex diffractometer with Cu anode using Co Kα radiation at 40 kV and 20mA over the range (2θ) of 5–80^o with a scan time of 1^o/min. Magnetization measurements were obtained at room temperature in magnetic fields up to 15 kOe using a vibrating sample magnetometer (Princeton Applied Research, model 4500). Fourier transform infrared (FTIR) spectra was recorded using KBr pellet technique on FTIR spectrometer Nicolet, Nesus 670.

Zeolite synthesis

Coal fly ash was used as starting material for zeolite synthesis by means of hydrothermal treatment. In synthesis experiment, 20 g of fly ash was heated to 100 ^{o}C in an oven for 24 h with 160 mL of 3.5 mol L^{-1} NaOH solution. The zeolitic material (ZC) was repeatedly washed with deionized water and dried at 100 ^{o}C for 24 h.

Preparation of the zeolite-iron oxide magnetic composite

Magnetite particles were prepared by adding of NaOH solution drop by drop into ferrous sulfate solution with agitation until the pH reached 11. The slurry was heated on a water bath. After that, the magnetite was washed with distilled water and dried at room temperature. The magnetite particles were redispersed in aqueous solution and zeolite synthesized from fly ash was added slowly with agitation. The zeolite/magnetite ratio was 3:1(w/w). The obtained zeolite-iron oxide magnetic composite (ZM) was washed with distilled water, dried at room temperature and milled**.**

Adsorption studies

The adsorption was performed by batch experiments. Kinetic experiments were carried out by agitating 5 mL of dye solutions of known initial dye concentration with 50 mg ZM at room temperature (25 ^{o}C) at a constant agitation speed of 360 rpm for 30-420 min in glass bottles. At timed intervals, the samples were placed on top of a magnet for 60 min to settle the particles, and 4 ml of supernatant was taken for the measurement. The concentration of dye in the supernatant solution was analyzed using a UV spectrophotometer (Cary 1E – Varian) by measuring absorbance at λ_{max} = 493 nm. Adsorption isotherms were carried out by contacting 50 mg of ZM with 5 mL of RO16 over the concentrations ranging from 1.2 to 20 mg L^{-1}. The agitation was made for 300 min, which is sufficient time to reach equilibrium. The amount of adsorption, q (mg g^{-1}), was calculated by:

$$q = \frac{V(C_o - C_e)}{W} . \quad (1)$$

where C_o and C_e (mg L^{-1}) are the liquid-phase concentrations of dye at initial and equilibrium time, respectively. V is the volume of the solution (L) and W is the mass of adsorbent used (g).

Results and Discussion

Characterization of the material

XFR measurement shows that the most of chemical compounds in ZM are iron (77.8%), silica (11.0%) and alumina (4.6%) with some calcium oxide (2.1%). The BET surface areas determined were 51.0 m^2 g^{-1} for zeolite-iron oxide magnetic composite ZM and 53.4 m^2 g^{-1} for zeolite ZC. The composite showed a decrease of BET surface area compared to the pure zeolite. The main reason for the surface area reduction in magnetic zeolite is due to the presence of the formed iron oxide, which has a smaller surface area compared to the pure zeolite.

The XRD analyses (Fig. 2) showed that hydroxysodalite (JCPDS-ICDD 00-011-0401) is the major phase in ZM with peaks of quartz and mullite of fly ash that remained after the treatment. A presence of a face-centered cubic (fcc) phase suggested to the presence of magnetite (JCPDS-ICDD 19-629).

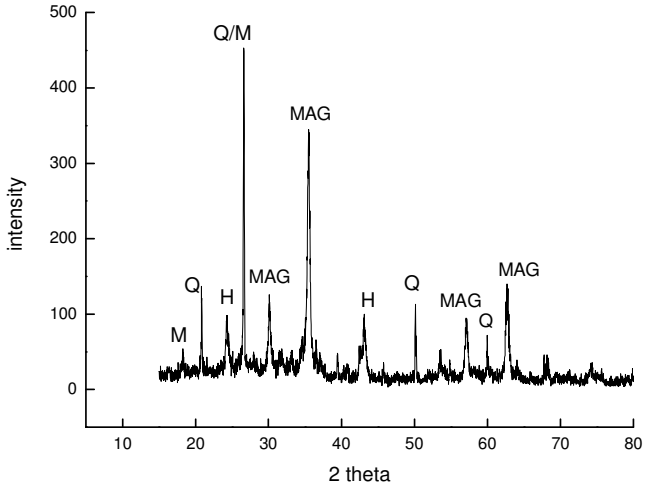

Figure 2. X-ray diffractogram for ZM. M = mulitte; Q = quartz; MAG = magnetite; H = hydroxysodalite.

As can be observed in Fig. 3, the magnetization curve measured for ZM showed no hysteresis. Neither coercivity nor remanence were observed and nanoparticle exhibited typical superparamagnetic behavior.

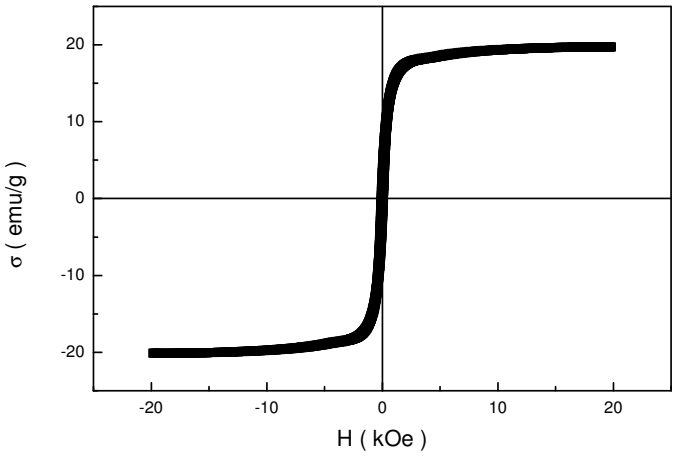

Figure 3. Magnetization curve of ZM.

The FTIR spectrum of ZM (Fig. 4) show the presence of magnetite nanoparticles by two absorption bands at around 631 and 561 cm^{-1}, which corresponds to the Fe–O bond of magnetite. The two broad bands at 3431 and 1642 cm^{-1} can be ascribed to the H_2O stretching vibration. An adsorption band was observed at around 992 cm^{-1}, which is assigned to the Al_2O/SiO_2 groups.

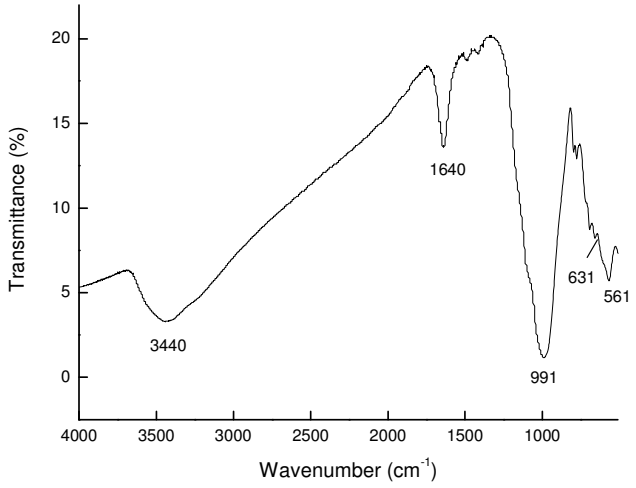

Figure 4. FTIR spectrum of ZM.

Effect of contact time

Figure 5 shows the dynamic adsorption of RO16 on ZM at initial concentration of 7.0 mg L^{-1}. The results showed that the extent of adsorption increased rapidly in the initial stages

before 60 min and then approaches equilibrium around 300 min. The amount of RO16 uptake is increasing with contact time. The removal curves obtained are single smooth and continuous suggesting the formation of a monolayer of adsorbate on the surface of the composite. During the initial stage of adsorption, a large number of vacant surface sites are available for adsorption. After a lapse of time, the remaining vacant surface sites are difficult to be occupied due to repulsive forces between the solute molecules on the solid surface and the bulk phase.

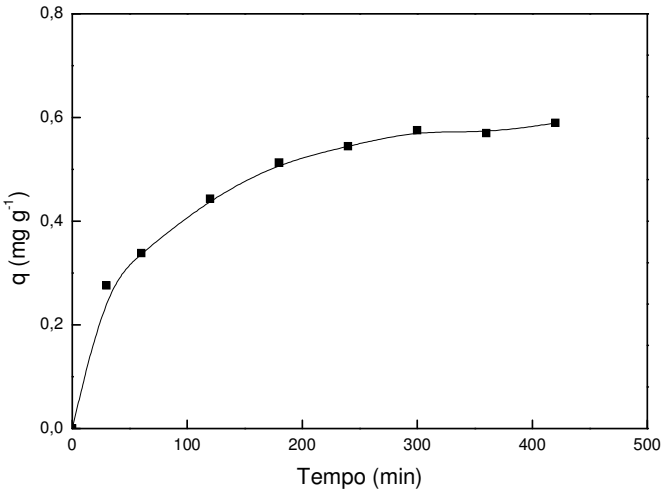

Figure 5. Dynamic adsorption of RO16 on ZM (C_o = 7.0 mg L^{-1})

Adsorption Kinetis models

Adsorption kinetics can be modeled by several models: pseudo-first-order kinetic; pseudo-second- order and intraparticle diffusion.

The pseudo-first-order model is given by [17]:

$$\log (q_e - q) = \log q_e - k_1 t / 2.303. \quad (2)$$

where q and q_e represent the amount of RO16 adsorbed (mg g^{-1}) at any time t (min) and at equilibrium time, respectively, and k_1 represents the adsorption rate constant (min^{-1}). Value of k_1 was calculated from the slope of the plot of log (q_e – q) versus t.

The kinetic data were further analyzed using a pseudo-second-order relation proposed by Ho *et al.* [18], which is represented by

$$\frac{t}{q} = \frac{1}{k_2 q_e^2} + \frac{t}{q_e} \cdot \quad (3)$$

where k_2 is the pseudo-second-order rate constant (g mg^{-1} min^{-1}) and q_e and q represents the amount of RO16 adsorbed (mg g^{-1}) at equilibrium and at any time t (min). The parameters q_e and k_2 can be determined from the slope and intercept of the plot of t/q versus t.

The constant k_2 is used to calculate the initial adsorption rate h (mg/gmin), at $t \rightarrow 0$ as follows:

$$h = k_2 q_e^2. \quad (4)$$

According to intraparticle diffusion model [19]:

$$q = k_i t^{0.5} + C. \quad (5)$$

where k_i is the intraparticle diffusion rate constant (mg g^{-1} $min^{-0.5}$) and C (mg g^{-1}) is a constant, which provide the measure of the boundary layer thickness. A plot of q (mg g^{-1}) versus $t^{0.5}$ ($min^{0.5}$) will be a straight line with a slope k_i and intercept C when adsorption mechanism follows intraparticle the diffusion process.

The calculated kinetic constants values and the corresponding linear regression correlation constants are given in Table 2.

Table 2. Kinetic parameters for the removal of RO16 onto ZM

Pseudo- first-order			
k_1 [min^{-1}]	R_1^2		
1.15 $x10^{-2}$	0.9954		
Pseudo- second-order			
k_2 [g/mg min]	h [mg/g min]	q_e [mg/g]	R_2^2
3.90 x 10^{-2}	1.29 $x10^{-2}$	0.659	0.9991
Intraparticle diffusion			
C	k_{i2}	R_{i2}^2	
[mg/g]	[mg/g $min^{0.5}$]		
0.251	2.83 $x10^{-3}$	0.9556	

As shown in Table 2, the correlation coefficient value obtained from pseudo-second-order kinetic (R_2^2) was found to be higher than for the pseudo-first-order (R_1^2) and intraparticle diffusion models (R_{i2}^2). The higher R_2^2 value confirms that the adsorption process can be better represented by the pseudo-second-order mechanism.

Adsorption isotherms

In the present investigation the equilibrium data were analyzed using the Freundlich and Langmuir isotherm. The linear form of the Langmuir expression may be written as:

$$C_e/q_e = 1/bQ_o + C_e/Q_o. \quad (6)$$

where q_e is the solid-phase adsorbate concentration at equilibrium (mg g^{-1}), C_e is the aqueous-phase adsorbate concentration at equilibrium (mg L^{-1}), Q_0 (mg g^{-1}) is the maximum amount of adsorbate per unit weight of adsorbent to form a complete monolayer on the surface, and b is the Langmuir isotherm constant (L mg^{-1}), related to the affinity of the adsorption sites.

The linearized form of the Freundlich equation can be written as follows:

$$\log q_e = \log K_f + 1/n\ (\log C_e). \quad (7)$$

where K_f [mg/g(L/mg)$^{1/n}$] and n are Freundlich constants related to adsorption capacity and adsorption intensity of adsorbents.

Thus the Freundlich constant K_f and n can be calculated from the intercept and slope of plot between log q_e and log C_e. Similarly a plot of C_e/q_e versus C_e gives a straight line of slope $1/Q_0$ and intercepts $1/Q_0b$.

Equilibrium data of RO16 onto ZM is shown in Fig. 6. The isotherm shapes are largely determined by the adsorption mechanism and can therefore be used to diagnose the nature of the adsorption [20]. Fig. 6 clearly shows that adsorption isotherms are L2 type. In L2-type isotherms, the adsorption of solute on the adsorbent proceeds until saturation. The adsorption was between 46% and 86% under the conditions studied.

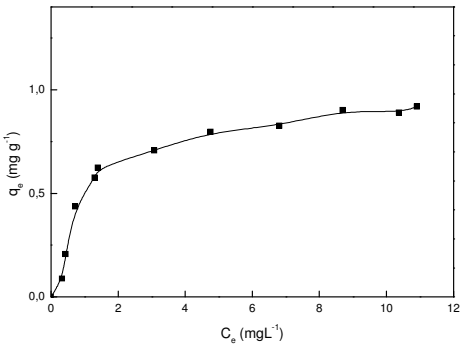

Figure 6. Adsorption isotherm of RO16 onto ZM (T = 25 ^{o}C).

The isotherm constants and correlation coefficients calculated for Freundlich and Langmuir equations are given in Table 3. It can be observed that the according the correlation coefficients criterion (R^2), equilibrium adsorption data followed Langmuir isotherm.

Table 3. Langmuir and Freundlich parameters for the adsorption of RO16 onto ZM39

Langmuir isotherm	
Q_0 (mg g ^{1})	1.06
b (L mg^{-1})	0.581
R^2	0.9843
Freundlich isotherm	
K_f [(mg g^{-1})(L $mg^{-1})^{1/n}$]	0.340
n	2.00
R^2	0.8736

Conclusion

The magnetic composite reported in this work combined the adsorption features of zeolite synthesized from fly ash with magnetic iron oxides. The zeolite-iron oxide magnetic nanocomposite is an effective adsorbent for the removal of azo dye Reactive Orange 16 from aqueous solution. Adsorption followed the Langmuir model with maximum adsorption capacity of 1.06 mg g^{-1}.

Acknowledgements

The support of Conselho Nacional de Desenvolvimento Científico e Tecnológico (CNPq), Brazil, is gratefully acknowledged. The authors are grateful to the Carbonífera do Cambuí Ltda. for supplying the coal ash samples.

References

[1] N.A., Booker, D. Keir, A. Priestley, C.D., Rithchie, D.L. Sudarmana and M.A. Woods: Water Sci. Technol. Vol. 23 (1991), p. 1703.

[2] M. Yamaura, R.L.Camilo and M.C.F C. Felinto: J. Alloys Compd. Vol. 344 (2002), p.152.

[3] M. Yamaura, R. L. Camilo, L.C. Sampaio, M.A. Macêdo, M. Nakamura and H.E. Toma: J. Magn. Magn. Mater. Vol. 279 (2004), p. 210.

[4] L.C.A. Oliveira, R.V.R.A. Rios, J.D. Fabris, V.K. Garg, K. Sapag and R.M. Lago: Carbon Vol. 40 (2002), p.2177.

[5] L.C.A. Oliveira, R.V.R.A. Rios, J.D. Fabris, K. Sapag, V.K. Garg and R.M. Lago: Appl. Clay Sci. Vol. 22 (2003), p. 169.

[6] L.C.A. Oliveira, D.I. Petkowicz, A. Smaniotto and S.B.C. Pergher: Water Res. Vol. 38 (2004), p. 3699.

[7] D.A. Fungaro, and M.G. Silva: Quím. Nova Vol. 25 (2002), p. 1081.

[8] D.A. Fungaro, M.S-M. Flues and A.P. Celebroni: Quím. Nova Vol. 27(2004), p. 582.

[9] D.A. Fungaro. J.C. Izidoro and R.S. Almeida: Eclética Química Vol. 30 (2005), p. 31.

[10] D.A. Fungaro and J.C. Izidoro: Quim. Nova Vol. 29, (2006), p. 735.

[11] T. Henmi: Clay Science Vol. 6 (1987), p. 277.

[12] X. Querol, A. Alastuey, A. Lopez-Soler, F. Plana, J.M. Andres, R. Juan, P. Ferrer and C.R. Ruiz: Environ. Sci. Technol. Vol. 31 (1997), p**.** 2527.

[13] C. Poole, H. Prijatama, and N.M. Rice: Miner. Eng. Vol. 13 (2000), p. 831.

[14] S. Rayalu, S.U. Meshram and M.Z. Hasan: J. Hazard Mater. Vol. B77 (2000), p. 123.

[15] P.K. Kolay, D.N. Singh, and M.V.R. Murti: Fuel Vol. 80 (2001), p. 739.

[16] N. Murayama, H. Yamamoto, and J. Shibata: Int. J. Min. Process, Vol. 64 (2002), p. 1.

[17] Y.S. Ho and G. McKay: Can. J. Chem. Eng. Vol. 76 (1998), p. 822.

[18] Y.S. Ho, D.A.J. Wase and C.F. Forster: Environ. Technol. Vol. 17 (1996), p. 71.

[19] W.J. Weber and J.C. Morris, Journal Sanit. Engin. Div. ASCE Vol. 89 (1963), p. 31.

[20] C.H. Giles, T.H. MacEwan, S.N. Nakhwa and D. Smith: J. Chem. Soc. London, (1960), p. 3973.